## SEMICONDUCTOR ULTRASOUND TREATMENT

Discovered in the late 1960s and extensively explored since the 1980s (1), the ultrasound stimulated processes in Ge, Si, and compound semiconductors attracted the attention of various research groups. It has been demonstrated that ultrasonic vibrations generated into crystal can stimulate numerous defect reactions and, as a consequence, benefit a design of electronic materials with improved and even superior characteristics. This new technological approach has become a powerful tool of defect engineering to improve performance and reliability of microelectronics devices.

Ultrasonic processing of semiconductors and relevant mechanisms are referred to as ultrasound treatment (hereafter the UST). UST effect is a stable improvement of material properties and device parameters after they are affected by the ultrasound. The UST method utilizes a fundamental concept in solids; it is based on a coupling of the ultrasonic vibrations with a system of point defects, both of impurity and native origin, interacting with the extended defects such as dislocations, grain boundaries, and precipitates to control their physical properties and to improve defect related material parameters. The UST method is based on a solid and well understood physical concept. Crystal defects and their complexes can exist in a stable, unstable, or metastable configuration. The bottom line of UST technology is that mechanical vibrations can "help" a system of crystal defects in reaching a favorable position which has the lowest total energy; therefore, this is the preferable, stable state. On the other hand, UST is a simple and intuitive approach. Many people have experience with a simple ultrasound treatment in their daily routine, maybe without noticing it. The following illustrative case reveals the utility of mechanical vibrations to solve a simple problem.

Consider gas bubbles in a liquid. Imagine you decided to have a soda and are trying to get rid of the gas bubbles, which are strongly attached to the glass walls, before you drink it. Tap your finger on the glass, and immediately, some of these tough bubbles will be released and float to the surface. What happened? Acoustic vibrations were generated in the glass and transferred their energy to the bubbles. This extra energy was enough to release trapped bubbles by breaking their molecular bonds of surface tension with the glass. This simple example is surprisingly similar to what ultrasound is doing to enhance defect passivation with hydrogenation in poly-Si films, a material for a new generation of active-matrix liquid crystal displays. It will be shown later that trapped atomic hydrogen can be released by UST and moved to proper positions at dangling bonds which improves the transport properties of electrons and holes. This process can eventually improve a thin-film transistor's leakage current and threshold voltage, critical parameters of a transistor's application.

This article describes the UST method and apparatus and also summarizes UST controlled defect reactions, relevant mechanisms, and application issues. Particular examples, dislocation gettering in II-VI semiconductors and enhanced hydrogenation in poly-Si thin films, provide a deeper insight into specific UST mechanisms.

### UST METHOD AND APPARATUS

Ultrasonic vibrations have to be delivered to a semiconductor material or electronic device to perform UST processing. Three different techniques to generate ultrasonic vibrations are applicable.

1. The most general method utilizes an external source of ultrasound, such as a resonance piezoelectric transducer. This UST technique has the advantage of non-

contact processing in an active device region at the front surface of the wafer and is applicable for large-scale materials and devices, such as 8 in. Si-wafers and more than 12 in. flat-panel displays. This UST approach is also compatible with conventional device processing steps: deposition, annealing, doping, and passivation. A schematic of the UST unit—a key element of large-scale UST stations—is shown in Fig. 1. Low-amplitude ultrasonic vibrations are generated into a UST object: a semiconductor wafer, thin film on a substrate, or a microelectronics device using a piezoelectric transducer operating in resonance vibration mode and coupled to a UST object. Typically, a circular transducer is driven by a generator and power amplifier adjusted to the first resonance of its radial or thickness vibrations. The resonance frequency varies from 20 kHz to 100 kHz for the radial vibration mode and can be extended into the MHz range using thickness vibrations. This frequency depends on the transducer geometry, vibration mode, and material of a piezoelectric transducer, and varies with UST temperature and amplitude. Adjusted to a resonance frequency, a UST transducer generates a maximum ultrasonic amplitude which is quantified by the value of the acoustic strain. The amplitude of acoustic strain is a ratio of the vibrating amplitude to a characteristic size of the transducer (e.g., diameter). In the UST technique, the acoustic strain typically does not exceed $10^{-4}$, corresponding to the acoustic power of a few W/cm$^2$. To provide effective UST processing, the acoustic strain is controlled with a calibrated sensor of acoustic vibrations (a noncontact UST probe). The UST temperature can be stabilized from room temperature to the Curie point of the transducer (350°C for commercial PZT-5A piezoceramics). A sample has to be placed on a UST chuck composed of one or more UST transducers and tightly pressed against a chemically polished transducer surface using a vacuum contact. A computer system controls in-situ and adjusts the following UST parameters: amplitude, frequency, and temperature, operating in a feedback loop with a noncontact UST probe and a non-contact infrared temperature sensor. This approach has been realized in a multitransducer UST station, which is capable of processing large-scale wafers by delivery of a quasi-homogeneous distribution of UST amplitudes and temperatures from a set of UST transducers to the 12 in. diagonal samples. The station can be scaled up simply by adding ultrasound transducers at a custom designed configuration of the UST chuck.

2. UST vibrations can be alternatively generated into material using the internal piezoelectric effect of a semiconductor. In this case, the ac voltage can be applied via electrodes oriented along specific crystallographic directions (e.g., along the C axis in a hexagonal crystal). The ac electric field generates intensive ultrasonic vibrations when its frequency (between 100 kHz and 20 MHz) is adjusted to the acoustic resonance of the sample. This method is limited to semiconductors with a high resistance and a noticeable piezoelectric constant (CdS, CdSe, $CdZnP_2$, and others). It also requires a special sample shaped in a form of the acoustic resonator.
3. Another UST approach is based on pulsed laser absorption. The absorption in a crystal of a short nano-second laser pulse (e.g., a ruby laser with a power density of the order $10^{12}$ W/cm$^2$) generates a set of ultrasonic pulses. These ultrasonic vibrations can be coupled with crystal defects and perform effective UST processing. In this technique, laser power density has to be carefully controlled to prevent the degradation of a material due to the creation of new crystal defects.

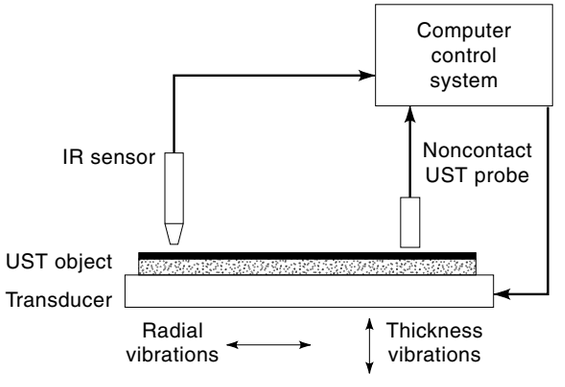


**Figure 1.** Schematic of ultrasound treatment unit for UST processing of semiconductor materials and devices.

## FUNDAMENTALS: UST PHENOMENA AND MECHANISMS

Although UST effects in semiconductors are well documented, there are a limited number of conclusive results where a clear understanding of the relevant physical mechanisms was achieved. Table 1 comprises a summary of UST mechanisms identified in various semiconductor materials. The key UST experiments, illustrating specific topics, will be discussed in detail.

UST mechanisms are tightly related to processes of point defect gettering. Defect gettering was introduced into semiconductors using the terminology of the cathode-ray-tubes, where the gettering technique is successfully applied to improve long-term vacuum characteristics of a tube with gas-absorbers. In Cz-Si microelectronics, a similar but essentially more sophisticated approach provided Si-wafers with a contamination level as low as $10^{11}$ cm$^{-3}$ (2). There are two general ways to achieve a high device yield and reliable device performance in IC technology. The first one requires a top-quality starting material which has to be processed further under an extremely clean fab environment. This is potentially a superior approach but at present it is not a realistic one. The second approach suggests the use of various defect engineering tools, particularly gettering and passivation to initially grow wafers with a moderate contamination level and to achieve a high-quality final product—the IC chip. According to a general gettering strategy, the gettering process is comprised of three consecutive steps: (1) release of a bound contamination impurity (Fe, Cu, Cr) introduced during wafer/device processing in a device region near the front surface of a wafer; (2) diffusion of released impurity toward the gettering sites (sinks) which are typically placed far away from the device region (e.g., at the back-side of the wafer surface), and (3) capture of contamination atoms at crystallographic defects or binding them with chemical elements at the gettering sites.

**Table 1. Ultrasound Stimulated Processes in Semiconductors**

| Physical Mechanism | Semiconductor | Reference |
|---|---|---|
| A. Capture of point defects | CdS | (3) |
| | CdTe | (4) |
| | ZnCdTe | (5) |
| B. Multiplication of dislocations | GaAs, GaP | (6) |
| | ZnCdTe | (5) |
| | Ge/GaAs | (7) |
| C. Dissolving of defect clusters and pairs | HgCdTe | (8) |
| | Cz-Si | (9) |
| | poly-Si films | (10,11) |
| | CdS | (12) |
| | GaAs | (13) |
| D. Enhanced diffusivity of point defects | Ge | (14) |
| | Si | (15) |
| | CdS | (16) |
| E. Metastable effects | Cz-Si | (9) |
| | GaAlAs | (17) |
| | GaAs | (18) |
| | CdS | (3) |

Two particular gettering processes—relaxation gettering and segregation gettering—can be implemented. The ability to control and facilitate any of the gettering steps can benefit the gettering efficiency. It was found that UST processing can positively affect each of three gettering steps: release, diffusion and capture, as will be illustrated below.

### Capture of Point Defects: Dislocation Gettering in II-VI

UST stimulated capture of mobile defects was experimentally observed in different II-VI semiconductors (Table 1). Point defect gettering benefits mechanical, transport, and optical properties of electronic material. The physical origin of UST gettering is a selective absorption of the ultrasound at extended crystal defects such as dislocations, grain boundaries, and precipitates. The energy of absorbed UST vibrations can be coupled with point defects to activate different defect reactions. We consider the vibrating string model of Granato-Lucke to describe a dislocation motion stimulated by ultrasound (19). This model is illustrated in Fig. 2. In this model, a dislocation line is considered as an elastic string oscillating between pinning points. It is assumed that for zero applied stress the dislocations are straight and pinned down by the impurity particles (a). In general, the concentration $c$ of impurity atoms on the dislocation line is larger than the overall concentration $c_O$ of impurities in the lattice, which is known as a dislocation Cottrell atmosphere. At temperature $T$ high enough for diffusion to take place, the concentration can attain an equilibrium value according to

$$c = c_O \exp(Q/kT) \tag{1}$$

where $Q$ is Cottrell interaction energy between a dislocation and impurity atom. In addition, it is assumed that the interaction of the dislocation with the lattice can be neglected as can interactions between individual dislocations. If an external low stress is now applied (b), the loops ($L_C$) start to bow out until the breakaway stress is reached. The effective modules of dislocation strain are determined by $L_C$ in this range. At the breakaway stress (c), a large increase in the dislocation strain occurs. For further increase of a stress, the network length $L_N$ bows out strongly, and these external stresses are critical for effective UST gettering. In fact, due to a dramatic increase of the dislocation strain in (c-d), the additional impurities can be swept out from the bulk and captured at the Cottrell atmosphere around the dislocation. It is suggested that both the elastic strain and electric field of the charged dislocation core are the driving forces in this UST gettering mechanism, contributing to the increase of the energy $Q$ in Eq. (1). Further increase of applied stress provides a multiplication of dislocations according to the Frank-Read mechanism (e). This process will be discussed later concerning the network of misfit dislocations. Dislocation motion can be monitored by measuring the internal friction coefficient which quantifies the value of dislocation ultrasonic damping. Internal friction study accesses the mechanical properties of a dislocation network such as the density of pinning points, length of dislocation segments, and breakaway stress.

The illustrative example of UST defect gettering is shown in Fig. 3 as two photoluminescence spectra measured in CdTe single crystals before UST and after UST processing (4). Low temperature PL spectroscopy is a convenient approach in selective monitoring of the concentration of point defects after various processing steps. Individual PL lines correspond to particular point defects possessing different electronic levels in a forbidden band. A variation of defect concentrations is ultimately reflected at the intensity change of corresponding PL lines. In Fig. 3, our concern is the intensity of two exciton

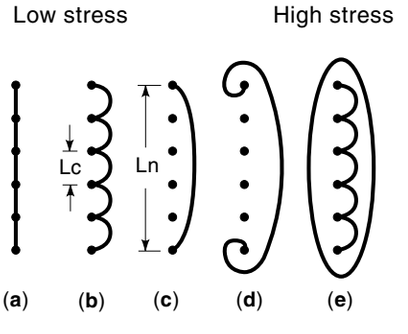


**Figure 2.** The successive drawings indicate schematically the bowing out of a pinned dislocation line by an increasing applied stress. As the stress increases, the loop $L_C$ bow out until breakaway occurs. For very large stresses, the dislocations multiply according to Frank-Read mechanism.

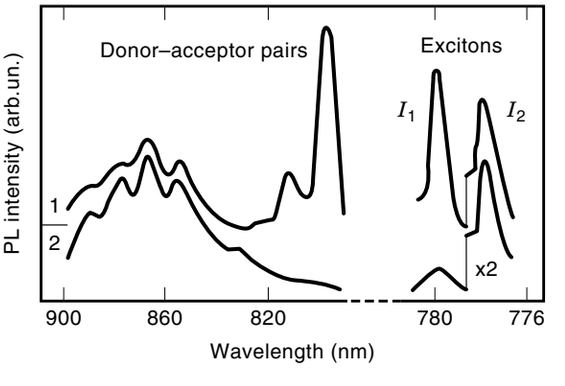


**Figure 3.** UST processing strongly reduces the concentration of shallow acceptors ($I_1$ line) and donor-acceptor pairs in CdTe single crystals. This is shown as two photoluminescence spectra of the same CdTe crystal measured at $T$ = 4.2 K before UST (1) and after UST (2).

lines: $I_1$ (acceptor exciton) and $I_2$ (donor exciton), and the donor–acceptor line with the principal maximum at 805 nm (1.54 eV). The UST obviously reduces the intensity of the acceptor excitonic line ($I_1$) and the donor–acceptor lines while barely changing the donor excitonic line ($I_2$). This UST process was identified as gettering of acceptor-type impurities: substitutional Li and Na. Similar UST results were obtained with gettering of Cu and Ag in CdTe and interstitial $Cd_I$ and $S_I$ in CdS (3). It was concluded that mobile point defects can be captured effectively by a dislocation network after UST processing. The PL spectroscopy data were approved by electrical measurements using thermally-stimulated conductivity. They are consistent with the results of internal fraction study: decrease of the internal friction coefficient after UST was observed in CdS single crystals. This result strongly suggests that the concentration of pinned points shown in Fig. 2 increased after UST processing, confirming the model of point defect gettering.

UST gettering can be an important technological approach in designing electronic materials with low contamination levels.

### Generation of Dislocations: Strained Ge Films on GaAs

Defect gettering is closely related to another important UST phenomenon: generation and multiplication of dislocations. In compound II-VI and III-V semiconductors, different types of dislocation—edge, screw, loop, and partial—are unavoidable growth and processing defects which strongly influence the electronic properties of materials. On the other hand, a promptly engineered dislocation network can benefit electronic materials, as was suggested by using misfit dislocations in the SiGe/Si system (2). In fact, dislocations in the vicinity of an active region can be an excellent sink to capture residual impurities and to accomplish defect gettering. Dislocations also provide a means to release a residual undesirable stress field at the misfit boundary between film and substrate. UST generation of dislocations occurs at a relatively high UST power density and is a result of a strong plastic deformation in the crystal lattice. Within a string model described previously [Fig. 2(e)], dislocations under strong UST stress can be released from some of their pinned points, and a dislocation multiplication will occur.

This process was directly observed using transmission electron microscopy in strained heterolayers composed of 0.2 $\mu$m to 5 $\mu$m Ge film deposited on a GaAs substrate (7). By applying UST processing for 3 h at 160 kHz with an acoustic strain amplitude of $2 \times 10^{-4}$, it was found that UST promotes the glide and multiplication of existing dislocations in a strained Ge/GaAs heterostructure. The following multiplication mechanism of misfit dislocations is schematically shown in Fig. 4. Initially [Fig. 4(a)], a straight 60° misfit dislocation AB oriented along the (110) direction is shown in the film-substrate boundary. Under UST [Fig. 4(b)], the dislocation dipole is formed in the (111) glide plane. This dipole can be broken by approaching a film surface [Fig. 4(c)], leaving two helical sections on the dislocation configurations AA′ and BB′. The misfit stresses cause these sections to glide transversely [Fig. 4(d)] and also in planes parallel to the original glide plane [Fig. 4(e)], lengthening the misfit dislocation segments and subsequently relaxing misfit stresses. When the helical segments reach the edges of the film, the final pattern of two

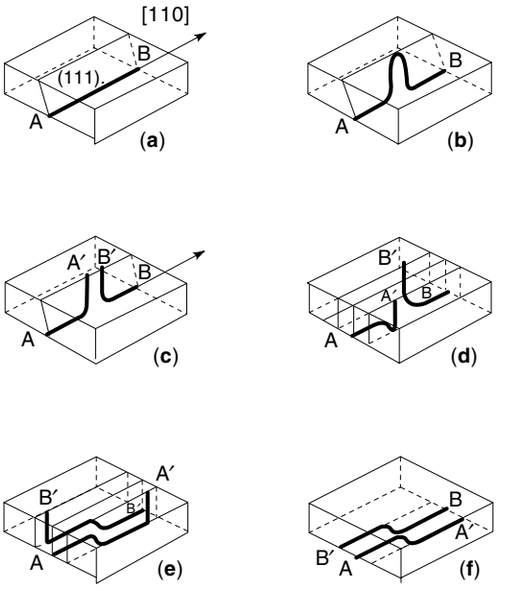


**Figure 4.** Schematic of consecutive stages of UST induced multiplication of the misfit dislocations at the heteroboundary between a thin film and substrate.

new misfit dislocations—AA′ and BB′—is designed. This elementary process of a dislocation multiplication can be repeated under UST and AA′ and BB′ dislocations. Consequently, a misfit dislocation network can be engineered.

We notice that dislocations are usually considered harmful defects in a semiconductor material or device. Therefore, special precautions have to be taken to avoid degradation of device performance after the dislocation network is created by UST. Methods of dislocation passivation, for example, using atomic hydrogen from a plasma source, as described later, can resolve this problem.

### Dissolving of Defect Clusters: Hydrogenation Enhancement in poly-Si

Polycrystalline silicon (poly-Si) thin films on glass or fused silica substrates are promising for thin film transistor (TFT) technology in active-matrix liquid crystal displays. Compared with transistors using amorphous silicon films, poly-Si TFTs have improved operational parameters due to substantially higher electron mobility. However, grain boundary states and interface defects in poly-Si lead to a high off-state current and affect the threshold voltage. A conventional approach to passivate these defect states and to reduce intergrain barriers for electron transport is to apply plasma hydrogenation. The hydrogen defect passivation occurs in two steps: plasma penetration and subsequent atomic hydrogen diffusion. Unfortunately, the diffusion of hydrogen in poly-Si is slow compared with single crystal silicon due to a trap limiting mechanism at grain boundaries, resulting in a long hydrogenation time (typically an hour at 300°C) and electrical inhomogeneity within passivated regions of poly-Si. This problem motivates a search for non-traditional approaches in order to improve hydrogenation in poly-Si films. It has appeared that the atomic hydrogen in poly-Si thin films is an especially suitable object for UST processes (10). Based on experiments, the

mechanism of UST enhanced liberation of the atomic hydrogen from trapping states was proposed (11). This UST effect is a "trigger" for fast hydrogen diffusion in poly-Si and ultimately provides an effective passivation of defects at grain boundaries.

For UST experiments, ultrasound vibrations were generated into 0.5 $\mu$m poly-Si films and thin-film transistors through a glass substrate using a circular 75 mm diameter piezoelectric transducer, as shown in Fig. 1. The UST transducer operated at about 25 kHz resonance of radial vibrations at temperatures ranging from room temperature to 300°C. The UST effect was monitored by measurement of a sheet resistance at room temperature using the four-point-probe method. Concurrently, spatially resolved PL and nano-scale contact potential difference mapping were performed.

It was found that conventional plasma hydrogenation applied to poly-Si films reduces the sheet resistance up to one order of magnitude due to hydrogenation of grain-boundary dangling bonds. In films where the plasma hydrogenation process was not completed, the additional strong reduction of resistance after UST by a factor of *two orders* of magnitude was observed (Fig. 5). It is important that resistance in non-hydrogenated films was practically not changed after the same UST. Another feature of the UST effect is an improvement of resistance homogeneity. By monitoring UST changes of the resistance in two different regions of the same film with a high starting electrical inhomogeneity, it was found that the initial difference in resistance of more than one order of magnitude was reduced to approximately 10% after a few consecutive steps of UST. Based on these findings, it was concluded that ultrasound vibrations applied to hydrogenated films promote a redistribution of the atomic hydrogen. This effect was directly observed by the measurement of contact potential difference mapping with a resolution of 20 nm. The contrast in contact potential mapping originating from the charge states at grain boundaries (non-passivated dangling bonds) was substantially improved after UST.

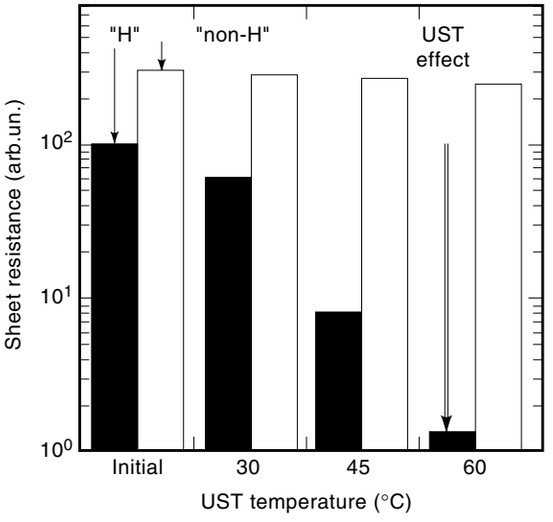


**Figure 5.** Effect of UST on the reduction of sheet resistance in plasma hydrogenated poly-Si thin film ("H") compared to non-hydrogenated film ("non-H"). UST parameters: acoustic strain $10^{-5}$, frequency 70 kHz, duration 30 min.

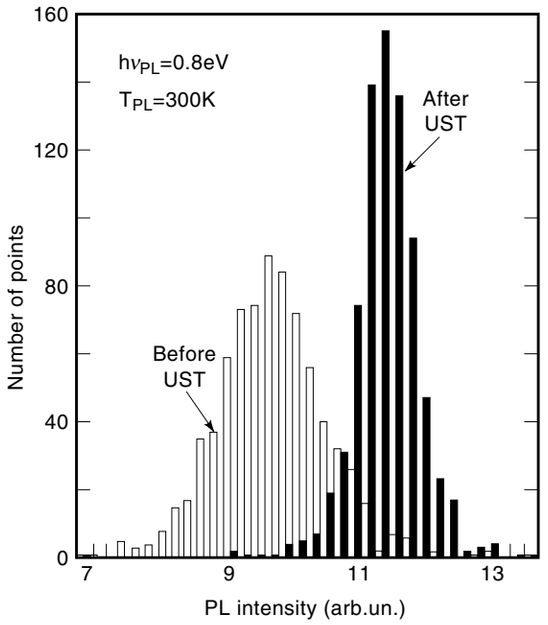


**Figure 6.** UST improves homogeneity of the photoluminescence intensity. PL mapping shows the increase of PL intensity and narrowing of the histogram in hydrogenated poly-Si film.

Photoluminescence (PL) spectroscopy accesses hydrogenation monitoring in poly-Si films. The PL intensity in poly-Si is increased after hydrogenation due to passivation of nonradiative centers: dangling silicon bonds at the grain boundaries. A spatially resolved PL mapping technique with a resolution of 100 $\mu$m was used to monitor UST distribution changes of recombination centers. The result is presented in Fig. 6 as two histograms of exactly the same hydrogenated film area prior to and after UST. The average value of PL intensity after UST exhibits an additional 30% increase and a narrowing of the histogram half-width by a factor of two (Fig. 6). This result is in excellent agreement with the UST-induced improvement of resistance homogeneity.

A dramatic UST effect was found in poly-Si films recrystallized from amorphous silicon (a-Si) at 550°C which contained a mixture of a-Si and poly-Si phases. A volume ratio of the crystalline to the amorphous phase was quantitatively measured by Raman spectroscopy. After UST was applied to films at $T_{UST}$ = 150 − 280°C, noticeable changes in the PL spectrum were observed (Fig. 7). Generally, the entire PL intensity was increased after UST. On the other hand, UST strongly activates a new broad PL band with a maximum at about 1.0 eV and a halfwidth of 0.26 eV. It is important that a dramatic enhancement of the 1.0 eV band exceeding *two orders* of magnitude requires only a few minutes of UST processing performed at 250°C. After UST activation of luminescence is completed, the PL spectrum is entirely dominated by the 1.0 eV band as shown in Figure 7. UST processing was performed at different temperatures between 150°C and 280°C, which allowed the evaluation of the activation energy of the UST effect, $E_{UST}$ = 0.33 eV. This value is an important parameter for the suggested UST model. It is important that this UST effect is stable: no relaxation was observed for a few months

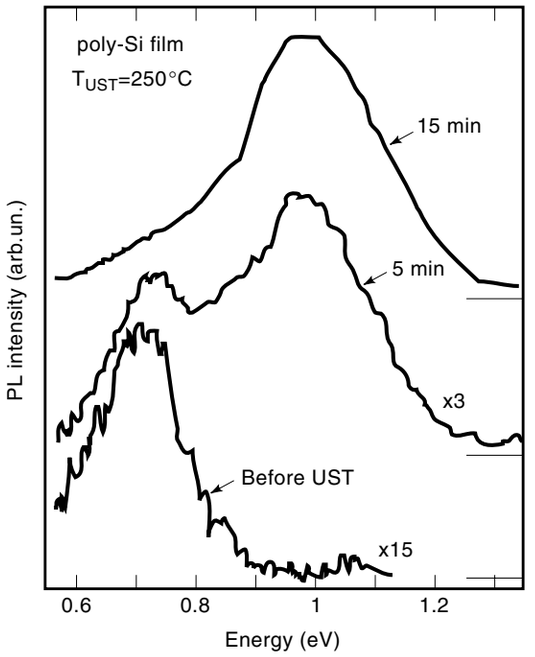


**Figure 7.** UST processing at 250°C for a few minutes exhibits a dramatic increase of luminescence intensity. This is due to passivation of nonradiative recombination centers with liberated atomic hydrogen.

within a temperature range from room temperature up to 300°C.

It is known that after plasma hydrogenation, the total hydrogen concentration in poly-Si films can exceed the number of nonpassivated dangling bonds by as much as two orders of magnitude. Therefore, a significant "reservoir" of electrically nonactive hydrogen in trapping states is available after plasma hydrogenation. It is suggested that UST promotes a release of hydrogen from traps (Fig. 8). A physical basis of such UST hydrogen detrapping is a selective absorption of the ultrasound by grain boundaries, dislocations, and other extended crystal defects where hydrogen can reside. Being liberated from traps, hydrogen subsequently become a fast diffuser with the diffusion coefficient of crystalline Si: $D_H = 9.4 \cdot 10^{-3} \times \exp(-0.48\ \text{eV/kT})$ [cm²/sec]. In fact, the measured UST activation energy ($E_{ust} = 0.33$ eV) has a value close to the activation of H diffusion in crystalline Si (about 0.48 eV). A possible reduction of this energy can be attributed to UST stimulated diffusion of the hydrogen, the UST mechanism discussed next. The diffusion length of hydrogen migration under UST ($T_{ust} = 280$°C, $\Delta t = 3$ min) can be estimated as $L = (D_H\ \Delta t)^{1/2} = 76\ \mu$m. This value substantially exceeds the 100 nm grain-size of poly-Si films, which explains why liberated hydrogen atoms can quickly approach the dangling bonds at grain boundaries of poly-Si. This is a remarkable similarity with the case of gas bubbles in a soda trapped on a glass wall and released after shaking off (see the beginning of this article).

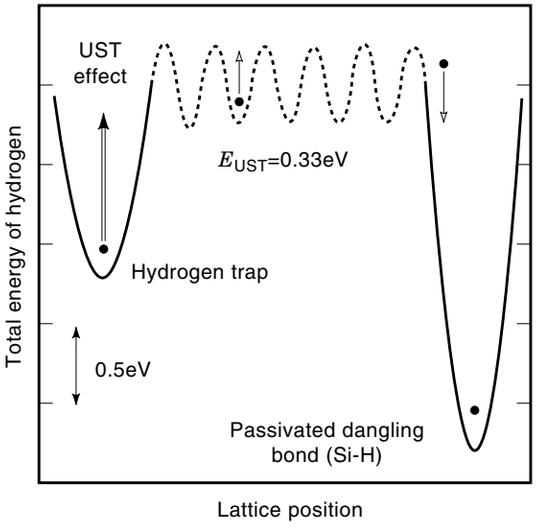


**Figure 8.** UST mechanism of enhanced passivation of dangling Si bonds consists of three consecutive steps: (a) UST release of the atomic hydrogen from traps; (b) fast hydrogen diffusion with activation energy of 0.33 eV; and (c) capture of hydrogen at dangling bond and forming of a stable Si-H complex.

UST processing was also applied to hydrogenated poly-Si thin film transistors. The reduction of a leakage current by a factor of 10, and a shift of the threshold voltage by as much as 0.5 V, are consistent with the proposed model of UST enhanced hydrogenation. These experiments demonstrate the utility of UST processing for the improvement of poly-Si active-matrix displays.

### Enhanced Diffusion: Cr in Cz-Si

Ultrasound accelerated diffusion of point defects was unambiguously observed first in metals, and after that, in semiconductor Ge and Si. UST reduces the activation energy of the diffusion process by a few tenths of an electron-volt, and by this means, it facilitates low-temperature defect reactions. This UST effect can potentially contribute to the gettering process.

UST enhanced diffusion is related to the multiplication of dislocations described above. In fact, diffusion of substitutional In, Al, and Ga in germanium single crystals was accelerated via a dislocation network. The mechanism is based on the fact that point defect diffusion is accelerated along the dislocation pipe compared with that in a regular crystal. This can be described by the equation

$$D_{UST}/D_0 = 1 + \pi r^2 N_D D_D / D_v \qquad (2)$$

where $D_0$ and $D_{UST}$ are the diffusion coefficients in the dislocation-free lattice and in UST dislocated crystals; $D_D$ and $D_v$ are the coefficients of diffusion via dislocation and in the volume of a crystal, $r$ is the radius of the dislocation pipe ranging from 1 nm to 10 nm, and $N_D$ stands for dislocation density. The ratio $D_D/D_v$ may exceed $10^6$, which explains the UST enhancement of point defect diffusivity in dislocated materials by a factor on the order of magnitude (14).

Diffusivity of point defects can also be facilitated in a dislocation-free material such as Cz-Si wafers. According to the theoretical model (20), the impurity atom absorbs the energy of nonequilibrium phonons excited by ultrasound, and this energy increases the rate of impurity migration. Two specific factors contribute to this UST mechanism: (1) the change in population of the impurity quantum oscillator levels due to the interaction of an impurity atom with ultrasonically ex-

cited non-equilibrium phonons, and (2) the change in the probability of an impurity migration at a particular quantum level.

Experiments were performed in p-type boron doped Cz-Si wafers codoped with Cr at concentrations from $10^{12}$ to $10^{-14}$ $cm^{-3}$ (21). In equilibrium, interstitial chromium atoms—$Cr_I$—form the nearest-neighbor Cr-B pairs which can be dissociated after 200°C annealing and quenching of the Si wafer. The following low-temperature pairing kinetics of $Cr_I$ and B is entirely controlled by $Cr_I$ bulk diffusion, which provides a convenient method of measuring the low-temperature diffusivity of the chromium ions. The rate of the Cr-B pairing can be measured at different temperatures from room temperature to about 100°C by monitoring pair concentration via the minority carrier diffusion length as a function of pairing time. The Arrhenius plot shown in Fig. 9 represents Cr diffusion data without UST and with UST. Measured in this way, the activation energy of $Cr_I$ diffusion without UST of 0.86 eV is consistent with published data. It is shown that this activation energy is significantly reduced by 0.27 eV under UST. This UST effect can potentially benefit gettering of Cr-contamination and improve commercial Si-wafers for IC applications.

Another example is provided by the UST enhanced diffusivity of donors in CdS single crystals, where the ultrasound was generated with a pulsed laser beam (16). The effect of shallow donor gettering by dislocations was substantially enhanced and occurred within a micro-second time frame, independent of the UST temperature between 77 K and 300 K. This was interpreted as an extremely low activation energy of point defect diffusivity under pulsed UST processing.

UST acceleration of defect diffusivity can be applied to different technological problems requiring fast defect reactions.

### Metastable Effects

Although UST phenomena are defined as a stable improvement of semiconductors and devices, a number of metastable effects mediated by ultrasound have been observed. Metastability is a general property of defects in electronic materials which are growing and are processed under nonequilibrium conditions (doping, passivation, annealing, etc.). Applying the low-amplitude ultrasonic vibrations to a system, one can perform nondestructive defect diagnostics by measuring post-UST relaxation of material characteristics and device parameters.

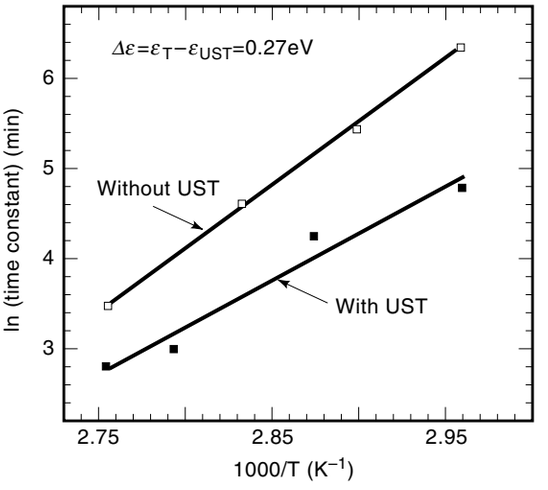


**Figure 9.** Ultrasound vibrations stimulate low-temperature diffusion of interstitial Cr in Cz-Si. UST reduces the activation energy of Cr diffusion to form Cr-B pairs.

An illustrative case follows which shows UST stimulated dissociation of Fe-B pairs in Cz-Si wafers (9). Contamination of commercial Si wafers with iron, even at the level of $10^{11}$ $cm^{-3}$, is detrimental for IC manufacturing. Therefore, a sensitive technique was developed for in-line control of Fe-contamination. This technique utilizes a surface photovoltage (SPV) method to measure minority carrier diffusion length in the bulk of a semiconductor (22). Briefly, SPV is a noncontact, real-time method of quantitatively analyzing heavy metals in wafers. The technique uses light pulses directed onto the wafer to generate excess minority carriers. These carriers diffuse to the surface and change the surface potential. A noncontact electrode placed above a Si wafer surface senses the photovoltage which is measured as a function of the light penetration depth into bulk silicon. The shorter the diffusion length, or the greater the contamination, the faster the photovoltage is decreased with increasing light penetration depth. Although the SPV technique typically measures the net contamination level, the Fe can be specifically identified using additional strong light illumination. This light from a lamp-source activates Fe by splitting the Fe-B pairs and eventually reduces the diffusion length from an initial value ($L_0$) to a new one ($L_1$). According to a simple theory, the concentration of Fe-B pairs can be calculated as follows:

$$[\mathrm{Fe}] = 1.05 \times 10^{16}(L_1^{-2} - L_0^{-2})(\mathrm{cm}^{-3}) \tag{3}$$

For UST experiments, boron doped Cz-Si wafers were contaminated with iron at a concentration of $1.5 \times 10^{14}$ $cm^{-3}$. This concentration was evaluated by means of an optical activation technique using Eq. (3). At room temperature in p-type material, the Fe is paired with doping acceptors (B) forming stable up to 200°C nearest neighbor Fe-B pairs, similar to the Cr-B pair in the previous section. UST performed at temperatures below 100°C at 70 kHz stimulates the process of Fe-B pair dissociation. This was controlled by reduction of the minority carrier diffusion length measured with an SPV technique as shown in Fig. 10. It is important that 200°C annealing of Si is required for thermal dissociation of Fe-B pairs. The UST enhanced dissociation is followed by a pairing of Fe and B due to a coulombic attraction of charged pair constituents and a fast diffusion of the interstitial Fe. Therefore, this UST triggered process is entirely reversible. This model case of Fe-B splitting under UST has the following explanation. A mobile Fe, bound with boron in the Fe-B pair, can exhibit a jump from one interstitial position to a nearest equivalent one. The jump rate is strongly stimulated when the frequency, $f$, of the applied ultrasonic vibrations is close to the resonance of pair reorientation followed by the equation:

$$2\pi f = \nu_0 \exp(-U/kT) \tag{4}$$

where $\nu_0$ is the lattice phonon frequency (typically on the order of $10^{12}$ $s^{-1}$), $T$ stands for UST temperature, and $U$ is the pair binding energy on the order of 0.5 eV. It is easy to check that at 70 kHz, Eq. (4) is fulfilled at 124°C, which is close to the range of applied UST temperatures. The breaking of an

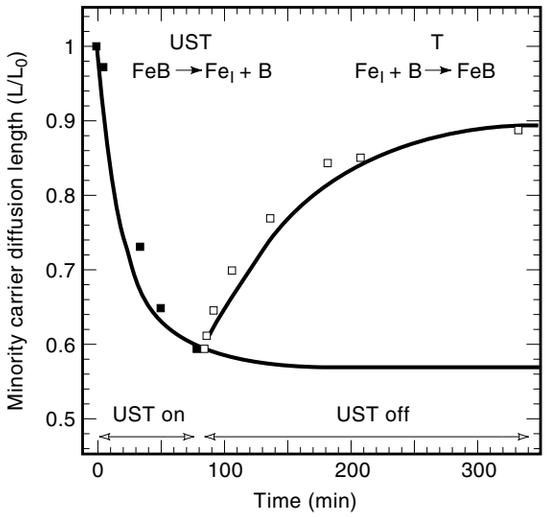


**Figure 10.** UST applied to *p*-type Cz-Si promotes breaking of Fe-B pairs. This process is monitored by a decrease of minority carrier diffusion length. After ultrasound is turned off, Fe and B are paired again, accomplishing reversible dissociation/association processes. UST breaking and pairing kinetics are measured at 75°C.

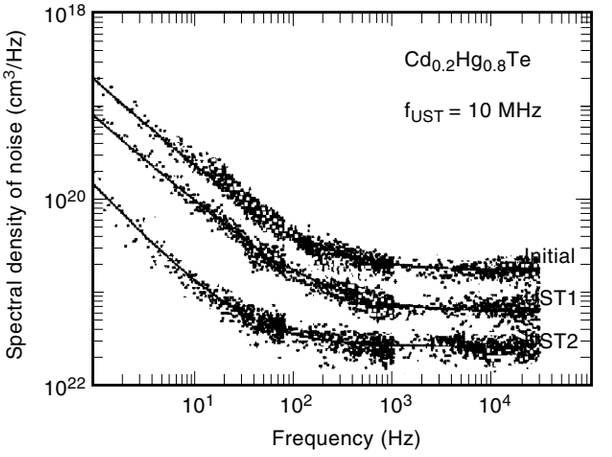


**Figure 11.** UST applied to CdHgTe ternary compound reduces the spectral density of $1/f$ noise by a factor of one order of magnitude (UST2) compared to the initial state. Further increasing of the UST intensity degrades the noise level to approximately the initial one.

Fe-B pair under UST occurs when the Fe atom approaches a saddle point between two equivalent interstitial sites; in this position, the coulombic binding energy is substantially reduced, which promotes a dissociation of the pair components.

Similar metastable UST phenomena were observed in II-VI materials (3,4). After the UST was accomplished, a long-term relaxation, measured at different temperatures, revealed diffusion of Cd interstitial atoms in CdS and shallow donors in CdTe. These kinds of experiments, UST dissociation ↔ thermal association of pair centers and defect clusters, can be used for other heavy metal contamination (Cu, W, Cr) in Si for the purpose of their selective diagnostics.

## UST APPLICATIONS

In Table 2, we summarized the results of UST applications in various semiconductor devices. The upper-limit of the UST effect shows the record of UST improvement of a device parameter. Some UST effects are indeed spectacular, while others just indicate a trend for follow-up research.

To illustrate one of the UST applications, a suppression of $1/f$ spectral density of noise in $Cd_{0.2}Hg_{0.8}Te$ polycrystalline material is shown in Fig. 11 (23). This material is a recognized leader among infrared detectors for commercial and military applications. Samples were cut from the *n*-type $Cd_{0.2}Hg_{0.8}Te$ slab containing small-angle boundaries. The $Cd_{0.2}Hg_{0.8}Te$ lattice is characterized by a high concentration of mobile point defects such as Hg vacancies, defect precipitates in the form of HgTe and Te inclusions, dislocations, and small-angle grain boundaries. This complicated defect system appeared to be a proper object for UST processing. The optimal UST effect was observed at an ultrasonic frequency in the range of 10 MHz, close to the characteristic vibration frequency of individual subblocks. UST was performed at room temperature, increasing the UST time from a few minutes to an hour. It is imperative to know that due to an extremely complicated combination of point and extended defects in a "soft" CdHgTe lattice, the UST effect is sensitive to experimental details, and even varies between samples cut from the same polycrystalline slab possessing different densities of small-angle grains boundaries. A dramatic, one order of magnitude reduction of the $1/f$ noise level (a critical parameter of IR sensitivity) is very impressive and promising for IR applications.

## SUMMARY AND CONCLUSION

We have reviewed fundamental and application issues of the UST method in various semiconductors and electronic de-

**Table 2. Improvement of Semiconductor Devices Using UST**

| Type of Device | Material | Improved Parameter | Upper Limit of UST Effect |
|---|---|---|---|
| Thin-film transistor | poly-Si film | leakage current | 10 times lower |
| Thin-film transistor | poly-Si film | threshold voltage | 0.5 V lower |
| Solar cell | crystalline poly-Si | quantum efficiency | 20% higher |
| Tunnel diode | GaAs | current noise | 4 times lower |
| Photodetector | CdSe | dark current | 100 times lower |
| Integrated circuit | Si | current noise | 2 times lower |
| Light emitting diode | In(Al)GaAs | intensity | 90% higher |

vices: single and compound materials; crystalline, polycrystalline, and amorphous; as-grown and processed wafers. Numerous ultrasonic-controlled defect reactions were observed and explored. Examples of a significant UST effect to enhance the point defect gettering and defect passivation with atomic hydrogen exhibit a strong potential for the UST technology to be utilized as a defect engineering tool.

After comprehensive study, UST mechanisms enabled the development of a reliable methodology and apparatus for using the UST in microelectronics and optoelectronics. Feasibility projects performed on semiconductor devices established a statistically valid database for applying this technique to benefit device performance. Although the core of UST technology—the generation of ultrasound into electronic material—is a common feature for various UST applications, a specific UST recipe has to be developed for each individual type of material or device. Such a recipe is comprised of a synergetic combination of the optimal UST parameters: temperature, amplitude, duration, and resonance frequency. Additionally, UST processing can be performed concurrently or consecutively with UV or IR light, under a pulsed electric field or laser activation, and so on. This illustrates a high level of flexibility of the UST technology, its compatibility with different stages of device fabrication, and an easy adjustment to a particular device problem.

Although UST has not yet found a commercial niche in a broad variety of potential applications, one can predict that the time is near when UST technology will be an effective means for defect engineering in semiconductors.

## BIBLIOGRAPHY


1. I. V. Ostarovskii and V. N. Lysenko, Generation of point defects under ultrasound in CdS, *Sov. Phys. Solid State,* **24**: 1206–1208, 1982.
2. F. Shimura, *Semiconductor Silicon Crystal Technology,* San Diego, CA: Academic Press, Inc., 1989.
3. A. P. Zdebskii et al., Mechanism of ultrasound-stimulated changes in photoelectric and luminescence properties of CdS, *Sov. Phys. Semicond.,* **20**: 1167–1170, 1986.
4. V. N. Babentsov et al., Influence of ultrasonic treatment on the exciton and impurity luminecence of CdTe, *Sov. Phys. Semicond.,* **25**: 749–750, 1991.
5. G. Garyagdiev et al., Mechanisms of ultrasound-induced changes in electrical and photoelectric properties of single crystals of ZnCdTe solid solutions, *Sov. Phys. Semicond.,* **25**: 248–250, 1991
6. D. Klimm et al., Ultrasonic treatment of GaP and GaAs, *Phys. Stat. Sol. (a),* **138**: 517–521, 1993.
7. V. F. Britun et al., Structural changes induced by ultrasound in stressed heterosystems, *Sov. Phys. Solid State,* **33**: 1317–1319, 1991.
8. P. I. Baranskii et al., Mechanism of changes in the carrier mobility due to ultrasonic treatment of semiconductor solid solutions, *Sov. Phys. Solid State,* **32**: 1257–1258, 1990.
9. S. Ostapenko and R. Bell, Ultrasound stimulated dissociation of Fe-B pairs in silicon, *J. Appl. Phys.,* **77**: 5458–5460, 1995.
10. S. Ostapenko et al., Enhanced hydrogenation in polycrystalline silicon films using low-temperature ultrasound treatment, *Appl. Phys. Lett.,* **68**: 2873–2875, 1996.
11. Y. Koshka et al., Activation of luminescence in polycrystalline silicon thin films by ultrasound treatment. *Appl. Phys. Lett.,* **68**: 2537–2539, 1996.
12. V. L. Gromashevskii et al., Acousto-chemical reactions in CdS, *Ukr. Fiz. Zhurnal,* **29**: 550–554, 1984.
13. A. Makosa, T. Wosinski, and Z. Witczak, Transformation of native defects in GaAs under ultrasonic treatment, *Acta Physica Polonica A,* **84**: 653–656, 1993.
14. V. P. Grabchak and A. V. Kulemin, Influence of ultrasound on the diffusion of impurity atoms and the dislocation structure in germanium single crystals, *Sov. Phys. Acoust.,* **22**: 475–478, 1976.
15. V. D. Krevchik, R. A. Muminov, and A. Ya. Yafasov, Influence of ultrasound on ionic diffusion process in semiconductors, *Phys. Stat. Sol. (a),* **63**: K159–K162, 1981.
16. L. V. Borkovskaya et al., Ultrasound-stimulated athermal donor motion in CdS cyrstals, *Phys. of the Solid State,* **37**: 1511–1513, 1995.
17. A. E. Belyaev et al., The ultrasonic-induced quenching of the persistent photoconductivity related to DX centers in AlGaAs, *Material Science Forum,* **143–147** (2): 1057–1061, 1994.
18. I. A. Buyanova et al., Ultrasound regeneration of EL2 centers in GaAs, *Semicond. Sci. Technol.,* **9**: 158–162, 1994.
19. A. V. Granato and K. Lucke, The vibrating string model of dislocation damping, in *Physical Acoustics,* W. P. Mason (ed.), **4A**: 225–276, 1966.
20. V. N. Pavlovich, Enhanced diffusion of impurities and defects in crystals in conditions of ultrasonic and radiative excitation of crystal lattice, *Phys. Stat. Sol. (b),* **180**: 97–105, 1993.
21. R. E. Bell, S. Ostapenko, and J. Lagowski, Ultrasound defect engineering of transition metals via metal-acceptor pairs in silicon, in *Defect and Impurity Engineered Semiconductors and Devices,* Pittsburg, PA: Material Research Society, 647–652, 1995.
22. J. Lagowski et al., Non-contact mapping of heavy metal contamination for silicon IC fabrication, *Semicon. Sci. Technol.,* **7**: A185–A192, 1992.
23. Y. M. Olikh and Y. N. Shavlyuk, Acoustically stimulated suppression of 1/f noise in subblock CdHgTe crystals, *Phys. of the Solid State,* **38**: 1835–1838, 1996.



SERGEI OSTAPENKO
University of South Florida

NADEJDA E. KORSUNSKAYA
Institute of Semiconductor Physics

MOISSEI K. SHEINKMAN
Institute of Semiconductor Physics

SERGEI KOVESHNIKOV
SEH America, Inc.


**SEMICONDUCTOR X-RAY LITHOGRAPHY.** See X-RAY LITHOGRAPHY.

**SENSING.** See TACTILE SENSORS.

**SENSING DEVICES, ELECTRIC.** See ELECTRIC SENSING DEVICES.